ENVIRONMENTAL TOXICOLOGY AND PHARMACOLOGY 34 (2012) 67–80

available at www.sciencedirect.com

ScienceDirect

journal homepage: www.elsevier.com/locate/etap

# Gene expression profiling of nephrotoxicity from copper nanoparticles in rats after repeated oral administration

*MingYang Liao, HuaGang Liu**

*GuangXi Medical University, 22 Shuang Yong Road, Nanning, Guangxi, PR China*

ARTICLE INFO

*Article history:*
Received 19 October 2010
Received in revised form 3 May 2011
Accepted 28 May 2011
Available online 13 June 2011

*Keywords:*
Copper nanoparticals
Nanotoxicology
Nephrotoxicity
Microarray
Toxicogenomics

ABSTRACT

The goal of this study was to investigate the mechanisms of nanocopper-induced nephrotoxicity by analyzing renal gene expression profiles phenotypically anchored to conventional toxicological outcomes. Male Wistar rats were given nanocopper (50, 100, 200 mg/kg) and microcopper (200 mg/kg) at different doses for 5 days. We found nanocopper can induce widespread renal proximal tubule necrosis in rat kidneys with blood urea nitrogen and creatinine increase. Whole genome transcriptome profiling of rat kidneys revealed significant alterations in the expression of many genes involved in valine, leucine, and isoleucine degradation, complement and coagulation cascades, oxidative phosphorylation, cell cycle, mitogen-activated protein kinase signaling pathway, glutathione metabolism, and others may be involved in the development of these phenotypes. Results from this study provide new insights into the nephrotoxicity of copper nano-particles and illustrate how toxicogenomic approaches are providing an unprecedented amount of mechanistic information on molecular responses to nanocopper and how they are likely to impact hazard and risk assessment.



## 1. Introduction

Nanoscience and nanotechnology are dynamically developing scientific fields throughout the world and have already become key research and development priorities in Europe and North America (Aguar-Fernandez and Hullmann, 2007; Zweck et al., 2008). Nanotechnology is often regarded as an 'enabling technology' (Mann, 2006). The use of nanotechnology in commercial applications is increasing in many scientific disciplines, including electronics, sporting goods, tires, stain-resistant clothing, cosmetics, and medicines for diagnosis, imaging, and drug delivery. With the ongoing commercialization of nanotechnology products, human exposure to nanomaterials will dramatically increase, and evaluation of their potential toxicity is essential. Several manufactured nanomaterials have recently been shown to cause adverse effects in vitro and in vivo (Donaldson et al., 2006; Lewinski et al., 2008; Medina et al., 2007), including copper nanoparticles (nanocopper) (Chen et al., 2006; Meng et al., 2007; Griffit et al., 2007, 2009).

Nanocopper has shown great promise as an osteoporosis treatment drug, antibacterial material, additive in livestock and poultry feed, and intrauterine contraceptive device. Furthermore, nanocopper has been widely used in industry, e.g., as an additive in lubricants (Liu et al., 2004), for metallic coating (Cioffi et al., 2005), and as a highly reactive catalyst in organic hydrogen reactions. A recent report demonstrated that when mice are acutely exposed to nanocopper or microcopper particles, only nanocopper particles induce severe impairment of the kidney, liver, and spleen (Chen et al., 2006). A further study revealed that the toxicity of nano-sized copper particles is highly correlated with the particle size/specific surface area. Compared to micro-copper (17 μm), nanocopper

* Corresponding author. Tel.: +86 771 5700208; fax: +86 771 5854772.
E-mail address: hgliu@263.net (H. Liu).
1382-6689/$ – see front matter © 2012 Published by Elsevier B.V.
doi:10.1016/j.etap.2011.05.014

(23.5 nm) can rapidly interact with artificial gastric acid juice and be transformed into ionic copper, which has ultrahigh reactivity. Moreover, metabolic alkalosis and copper accumulation in the kidneys were detected in mice that were orally exposed to nanocopper particles (Meng et al., 2007). However, the characteristics of nanocopper-induced subacute toxicity in repeatedly exposed rats and the mechanism of its nephrotoxicity at the molecular level remain unclear. A study of repeated exposure to nanocopper is more similar to the conditions of exposed humans, and investigation of the mechanism of nanocopper toxicity will provide information important in preventing and reducing the toxicity of nanocopper.

Our study design is based on the framework systems toxicology and the different levels of -omics data, including transcriptomics, proteomics, and metabonomics, which will be integrated and anchored to the phenotype of traditional toxicology, finally leading to a systems toxicology understanding of nanocopper. Here, we focused on the gene expression profiles of nanocopper-exposed rat kidneys, because evaluation of gene expression in affected tissues is important for providing 'high coverage' of possible targets and drawing inferences about affected circuitry. We treated animals with nanocopper or micro-copper at different doses for 5 days. The gene expression profiles of rat kidney and conventional toxicological parameters including body weight, clinical chemistry, and histopathology were examined to gain more insight into the characteristics of the subacute toxicity of nanocopper and the molecular mechanism of its nephrotoxicity at the genomic level.

## 2. Materials and methods

### 2.1. Physicochemical characterization

Commercial-grade copper nanoparticles (25 nm) were purchased from Shenzhen Zunye Nano Material Co. Ltd. (Shenzhen, China). Micro-copper particles (200-mesh) were purchased from Beijing HaoYun Co. Ltd. Before the experiment, the size distribution, specific surface area, and impurities were analyzed. The size distribution of 25-nm copper particles in a 1% (w/v) hydroxypropylmethyl cellulose (HPMC) solution (K4M, Shanghai Colorcon Coating Technology Ltd., China) was analyzed with a dynamic light scattering particle size analyzer (LB-550 HORIBA, Japan) and atom force microscopy (Daojin Co., Japan). The specific surface area was determined with a BET surface area analyzer (ASAT 2020 M+C Micromeritics, USA). Impurities (e.g., aluminum, barium, calcium, chromium, chrome, iron, magnesium, manganese, molybdenum, sodium, etc.) were analyzed with X-ray fluorescence spectroscopy. The dissolution of 25-nm Cu in the administered solution was performed with inductively coupled plasma-atomic absorption spectrometry (ICPAAS-7000, Daojin Co., Japan). Copper particle suspensions were prepared as described (Chen et al., 2006).

### 2.2. Animals

All animal studies were approved by the Ethics Committee of Animal Care and Experimentation of the National Institute for Environmental Studies, China. Seven-week-old male Wistar rats were purchased from Weitong-Lihua Experimental Animal Center, (Beijing, China) and housed in stainless-steel cages in a 12 h light/dark cycle, ventilated with an air-exchange rate of 15 times/h, and maintained at 21–25 °C with a relative humidity of 40–70%. Each animal was allowed free access to water and pellet food.

### 2.3. Experimental design

After a 7-day quarantine and acclimatization period, the animals were divided into groups of six animals each with a computerized stratified random grouping method based on body weight (BW). The groups included HPMC (vehicle control), 200 mg/kg microcopper, and 100 mg/kg and 200 mg/kg nanocopper. According to the $LD_{50}$ = 834.3 mg/kg obtained from our previous acute toxicity test, the high dose of nanocopper was determined by a 1-week dose-finding study (data not shown), and subsequently, the low dose was determined to be 100 mg/kg. To observe the size effect of nanotoxicity, 200 mg/kg microcopper was selected. Animals were orally gavaged with the nanocopper or microcopper suspended in 1% (w/v) HPMC solution daily for 5 consecutive days. Control rats were administered a similar volume of 1% HPMC. The selection of route of administration was based on the fact that nanocopper used to treat osteoporosis is taken orally. For conventional toxicological parameters, data collected included BW, clinical chemistry (blood urea nitrogen [BUN] and creatinine [Crn]), and microscopic pathology. For the '-omic' study, three portions of each liver and left kidney were isolated separately for use in transcriptomic, proteomic, and metabonomic analyses. Here, we focused on the gene expression profiles of nanocopper-exposed rat kidneys. Microarray analysis was conducted on three of the six samples from HPMC (vehicle control), 200 mg/kg microcopper, and 100 mg/kg and 200 mg/kg nanocopper groups with a GeneChip® Rat Genome 230 2.0 Array (Rat 230 2.0).

### 2.4. Body weight, clinical chemistry, and kidney histopathology

The BW of each animal was measured every day before administration. Blood samples were taken with a needle and heparinized syringe from the abdominal artery of animals under ether anesthesia 24 h after repeated dosing. Plasma biochemical assessments were conducted with a HITACHI 7020 Automatic Analyzer. After collecting the blood, the animals were euthanized under ether anesthesia by exsanguination from the abdominal veins and arteries. Liver and kidneys were collected from each animal and weighed. Three portions of each kidney were isolated and immediately frozen in liquid nitrogen and stored separately at −80 °C for use in transcriptomic, proteomic, and metabonomic analyses. The remaining samples were fixed in 10% buffered formalin solution for routine histological processing. Paraffin sections were stained with hematoxylin and eosin for histopathological examination and were graded as – (no change), ± (minimal), + (slight), ++ (moderate), and +++ (severe).

### 2.5. RNA extraction

Total RNA was isolated from kidneys with Trizol reagent (Invitrogen, Carlsbad, CA, USA). RNA was further purified with QIAGEN RNeasy mini columns (QIAGEN, Valencia, CA, USA) and resuspended in 50 μL diethylpyrocarbonate-treated water according to the manufacturer's protocol. The quality of the total RNA was evaluated by measuring the A260:A280 ratio, which ranged between 1.8 and 2.1. RNA integrity was examined by agarose gel electrophoresis and spectrophotometric analysis.

### 2.6. Microarray gene expression analysis

Microarray analysis was conducted on three of the six samples from each group with a GeneChip® Rat Genome 230 2.0 Array (Rat 230 2.0) (Affymetrix, Santa Clara, CA, USA), which includes over 31,000 probe sets representing approximately 28,700 well-substantiated rat genes. The procedure was conducted basically according to the manufacturer's instructions. Briefly, 5 μg of total RNA was used to synthesize cDNA with the Superscript Choice System (Invitrogen) and the T7-(dT)24-oligonucleotide primer (Affymetrix). After the cDNA was purified with a cDNA Cleanup Module (Affymetrix), biotin-labeled cRNA was synthesized with the bioarray high yield RNA transcript labeling kit (Enzo Diagnostics, Farmingdale, NY, USA). The cRNA was purified with an IVT cRNA Cleanup Spin Column (Affymetrix) and then fragmented. Twenty micrograms of the fragmented cRNA was hybridized to a RAE230A probe array for 18 h at 45 °C at 60 rpm. After hybridization, the array was washed and stained with streptavidin-phycoerythrin with the Fluidics Station 400 (Affymetrix). Finally, the array was scanned with a Gene Array Scanner (Affymetrix). The digital image files were processed with Affymetrix Microarray Suite version 5.0.

The hybridization data were analyzed with GeneChip Operating software (GCOS 1.4). The scanned images were first assessed by visual inspection and then analyzed to generate raw data files saved as CEL files using the default setting of GCOS 1.4. A global scaling procedure was performed to normalize the different arrays with dChip software. In a comparison analysis, we applied a two-class unpaired method in the SAM (Significant Analysis of Microarray) software to identify significantly differentially expressed genes between the test group and control group. First, probes with a raw intensity value >60 were selected to eliminate those with an intensity value close to background levels. Second, one-way analysis of variance (ANOVA) was performed with a parametric test assuming equal variances and Benjamini and Hochberg as multiple testing corrections with a False Discovery Rate of 0.01. This ANOVA analysis was used to select genes that were significantly differentially expressed in at least one of the pairwise comparisons, ensuring that the differences were due to the treatment, not chance. This procedure also filtered out genes without any changes across the experimental conditions. Results for comparison pairs are expressed as a fold change. Statistical significance was assigned as a minimum 2-fold change and $P < 0.05$.

For designing experiments involving microarrays, we adhered to the Minimum Information About a Microarray Experiment (MIAME) guidelines developed by the Microarray Gene Expression Data Society (http://www.mged.org/miame).

### 2.7. Volcano plots and clustering

Volcano plots were used to visually compare the size of the fold change to the statistical significance level of the genes between control and nanocopper- and microcopper-exposed rats. Average linkage clustering analysis based on centered Pearson correlation was implemented in the Cluster program and Java Tree view 1.0.12® software (Eisen et al., 1998).

### 2.8. Gene ontology and pathway enrichment

All differentially expressed genes were analyzed with a free web-based Molecular Annotation System 2.0 (MAS 2.0, http://bioinfo.capitalbio.com/mas/), which integrates GO(Gene ontology) and 3 different open source pathway resources: KEGG, BioCarta, and GenMAPP. In the MAS 2.0 tool, the pathways are ranked with statistical significance by calculating their *P*-values based on hypergeometric distribution.

### 2.9. Real-time Quantitative PCR validation of gene expression

To confirm the Affymetrix gene array data, real-time quantitative PCR was performed. PCR primers and probes were designed with Primer3 v3.0 Software (http://frodo.wi.mit.edu/). The mRNA level of *Gapdh* was used as an internal control, and gene-specific mRNA expression was normalized to *Gapdh* expression. Forward (F) and reverse (R) primers used are listed in Table 1. Total RNA was isolated with Trizol reagent (Invitrogen), and cDNA was generated with reverse transcription using 1 μg of total RNA and the ImProm-IITM Reverse Transcription System (Promega, Madison, WI, USA). Quantitative real-time PCR was performed on an MX 3000P™ PCR Instrument (Stratagene, San Diego, CA, USA) using SYBR Premix EX TaqTM (TaKaRa, Dalian, China). PCR parameters were as follows: 10 s at 95 °C, and then 40 cycles of 5 s at 95 °C and 20 s at 60 °C. Each sample was tested in triplicate. Threshold values were determined for each sample/primer pair, and average and SE values were calculated. The PCR products were verified by melting curve analysis.

### 2.10. Additional statistical analysis

Data are presented by descriptive analysis as the mean ± standard deviation (S.D.) of 6 animals. Statistical analysis for the animal weights and clinical biochemistry was performed with SPSS 13.0 software. The distribution of the data was checked for normality with the Shapiro-Wiks test. The homogeneity of the variance was verified with the Levene test. The comparisons were performed using one-way ANOVA followed by a Dunnett's test, and a *p*-value below 0.05 was considered significant.

**Table 1 – Sequences of primer sets for real-time quantitative PCR.**

| Gene symbol | Gene description | Primer sequences (5′–3′) |
|---|---|---|
| *Gapdh* | Glyceraldehyde-3-phosphate dehydrogenase | F ACAGCAACAGGGTGGTGGAC |
| | | R TTTGAGGGTGCAGCGAACTT |
| *Kim1* | Kidney injury molecule 1 | F CGCAGAGAAACCCGACTAAG |
| | | R CAAAGCTCAGAGAGCCCATC |
| *Gpx2* | Glutathione peroxidase 2 | F TGCCCTACCCTTATGACGAC |
| | | R TCGATGTTGATGGTCTGGAA |
| *Hspa1a* | Heat shock 70kD protein 1A | F GTCTCAAGGGCAAGATCAGC |
| | | R CTAGCCAACACCCTGAGAGC |
| *G6pc* | Glucose-6-phosphatase, catalytic | F GACCAGCCCGTGTAATGAGT |
| | | R AAGGTGGTGGTTCCTGAGTG |
| *Rgn* | Regucalcin | F TCAAAGACTGTCTGCCGATG |
| | | R TATCTCCCAGCAGGATCCAC |
| *F2* | Coagulation factor II | F ATGGCAGGTGATGCTTTTTC |
| | | R AGGGTGGGTACAGAATGCAG |

**Table 2 – Physicochemical parameters of nano-copper and micro-copper.**

| Particles | Average size | Size distribution | Particle number ($\mu g^{-1}$) | BET surface area ($m^2/g$) | Purity (%) |
|---|---|---|---|---|---|
| Nano-copper | 25 nm | 5–60 nm | $1.55 \times 10^{10}$ | 6.92 ± 0.03 | 99.9 |
| Micro-copper | 17 μm | 0.5–38 μm | 44 | 0.25 ± 0.03 | 99.9 |

## 3. Results

### 3.1. Physicochemical characterization

The physicochemical characterization results are summarized in Table 2. The results for nanocopper both with and without 1% HPMC indicated little influence of the inert suspension agent on the particle size and surface property of nanoparticles. The dissolution rate of the nanocopper particles was 0.014 ± 0.002% in 1% HPMC suspension solution following a 30-min ultrasonication.

### 3.2. General toxicity

Symptoms of gastrointestinal dysfunction, such as anorexia and severe diarrhea, were observed in all rats that were given a 200 mg/kg nanocopper dose. Drowsiness, hypopnea, tremors, and arching of the back were observed in four of the six rats. No abnormalities were observed in the other treated groups or the control group during the study period.

### 3.3. Conventional toxicological parameters

After 5-day repeated administration, the rats that were given 200 mg/kg nanocopper showed a dramatic weight loss (Table 3). For clinical chemistry measurements, 200 mg/kg/day of nanocopper significantly induced increases in BUN and Crn levels. For microcopper and 100 mg/kg/day nanocopper, no obvious increase in these parameters was detected (Table 4). Histopathological findings of the kidney in all rats (6/6) given 200 mg/kg nanocopper indicated widespread renal proximal tubule necrosis both in the pars convoluta and pars recta involving most of the nephrons. Further, cellular fragments were found in the tubule lumen, where orange crystal matter deposition was commonly observed (Fig. 1). Micro-copper (200 mg/kg) and nanocopper (100 mg/kg) only induced swelling of the proximal tubule epithelia in 4/6 and 6/6 rats, respectively. The histopathological grade evaluation of the kidney specimens is shown in Table 5.

### 3.4. Gene expression changes

The results of the global gene expression analysis provide insight into how gene expression in the kidneys of rats responded to treatment with nanocopper. Compared to the vehicle control group, 2773 genes were found to be differentially expressed in the 200 mg/kg nanocopper group, including 1060 genes that were upregulated and 1713 genes that were downregulated. In the 100 mg/kg nanocopper group, there

**Table 3 – Effects of nano-sized copper on body weight gain and organ weights (mean ± SD).**

| Group | Control | Micro-copper 200 mg/kg | Nano-copper (mg/kg) | |
|---|---|---|---|---|
| | | | 100 | 200 |
| Bodyweight gain (g) | 5.50 ± 5.79 | 4.86 ± 6.22 | 0.83 ± 11.67 | −54.33 ± 15.24** |

** $p < 00.01$ ($n = 6$ for all groups).

**Table 4 – Effects of nano-sized copper on serum clinical chemistry parameters(mean ± SD).**

| Parameters | Control | Micro-copper 200 mg/kg | Nano-copper (mg/kg) | |
|---|---|---|---|---|
| | | | 100 | 200 |
| BUN (mM/l) | 5.23 ± 0.84 | 6.34 ± 0.78 | 6.66 ± 1.98 | 28.09 ± 10.54** |
| Crn (μM/l) | 22.63 ± 3.65 | 23.87 ± 3.24 | 23.50 ± 4.39 | 270.63 ± 97.77** |

** $p < 0.01$ ($n = 6$ for all groups).

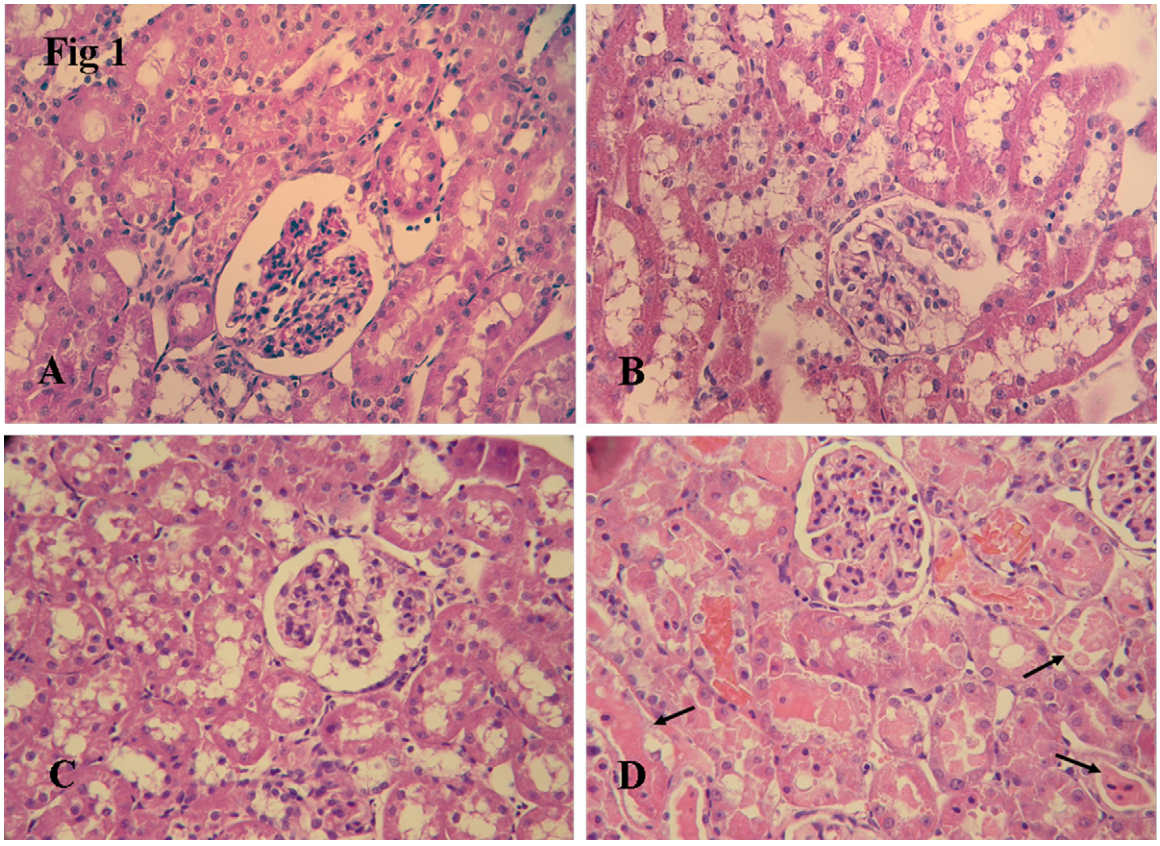


**Fig. 1 – Kidney histopathology of rats dosed nano-copper particles (HE stain). Magnification, 400×. (A) Control rats, with no abnormalities were noted. (B) Micro-copper particles (200 mg/kg/d) and (C) Low-dose (100 mg/kg/d) nano-copper-treated rats, the swelling proximal tubule was observed. (D) High-dose nano-copper-treated (200 mg/kg/d) rat, the widespread proximal tubular necrosis, orange crystal matter were noted.**

were 108 genes that changed dramatically, including 49 upregulated and 59 downregulated genes. In the microcopper group, only two genes changed dramatically. A review of the differentially expressed genes after treatment with 100 mg/kg nanocopper revealed 56 genes whose expression was also differentially regulated in response to the 200-mg/kg dose. The numbers of probe sets with altered expression are shown in Fig. 2.

**Table 5 – Histopathological evaluation of kidney specimens by grade.**

| Exp. group | Rat number | | | | | |
|---|---|---|---|---|---|---|
| | No. 1 | No. 2 | No. 3 | No. 4 | No. 5 | No. 6 |
| Vehicle control | – | – | – | – | – | – |
| Micro-copper (200 mg/kg/day) | + | ± | – | – | ± | ± |
| Nano-copper (100 mg/kg/day) | ± | + | ± | ± | ± | ± |
| Nano-copper (200 mg/kg/day) | +++ | +++ | +++ | +++ | ++ | +++ |

– (no change), ± (minimal), + (slight), ++ (moderate), and +++ (severe).

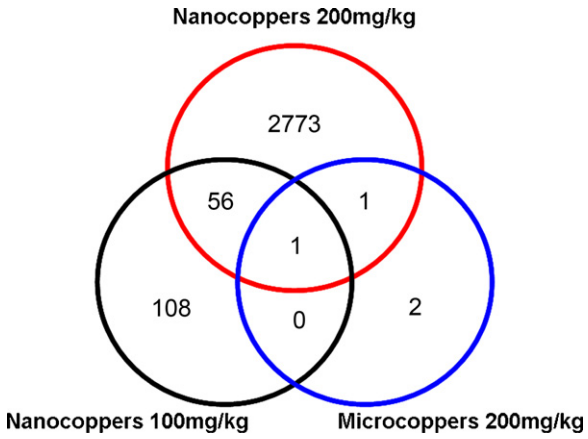


**Fig. 2 – A Venn diagram depicting differences and commonalities in the number of genes expressed following each exposure condition. Differentially expressed genes for nano-copper and micro-copper relative to vehicle control were used in developing the Venn diagram.**

### 3.5. *Volcano plots*

Volcano plots were constructed by comparing kidney samples from microcopper-treated or nanocopper-treated rats with samples from vehicle-exposed rats (Fig. 3). The 'volcano plots' arrange genes along dimensions of biological and statistical significance to compare the size of the fold changes to the statistical significance level. The first (horizontal) dimension is the fold change between the two groups (on a log scale, so that upregulated and downregulated genes appear symmetric), and the second (vertical) axis represents the *p*-value from a t-test of differences between samples (conveniently on a negative log scale, so that smaller *p*-values appear higher). The first axis indicates the biological impact of the change; the second indicates the statistical evidence. Fig. 3 shows differentially expressed genes between the 200 mg/kg nanocopper group and the vehicle control group. Red points represent genes that were upregulated more than 2-fold and with $P < 0.05$. Green points represent genes that were downregulated more than 2-fold and with $P < 0.05$.

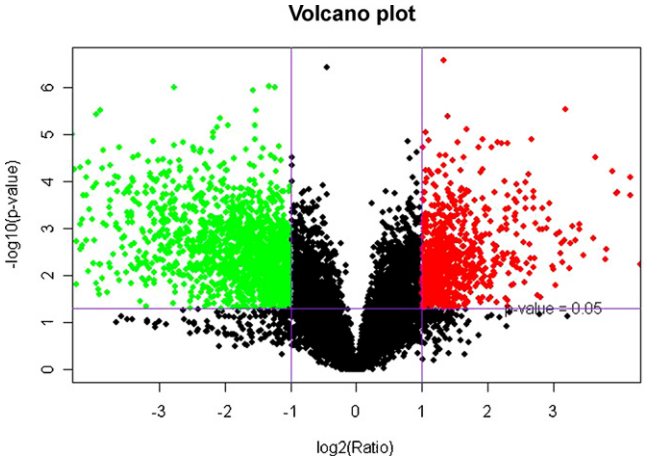


**Fig. 3 – Volcano plot displayed the differentially expressed genes between nanocoppers 200 mg/kg group and vehicle control group. The horizontal axis indicates biological impact of the fold change; the vertical indicates the statistical evidence. Red points represents the genes up-regulated more than 2 fold and $P < 0.05$. Green points represents the genes down-regulated more than 2 fold and $P < 0.05$. (For interpretation of the references to colour in this figure legend, the reader is referred to the web version of this article.)**

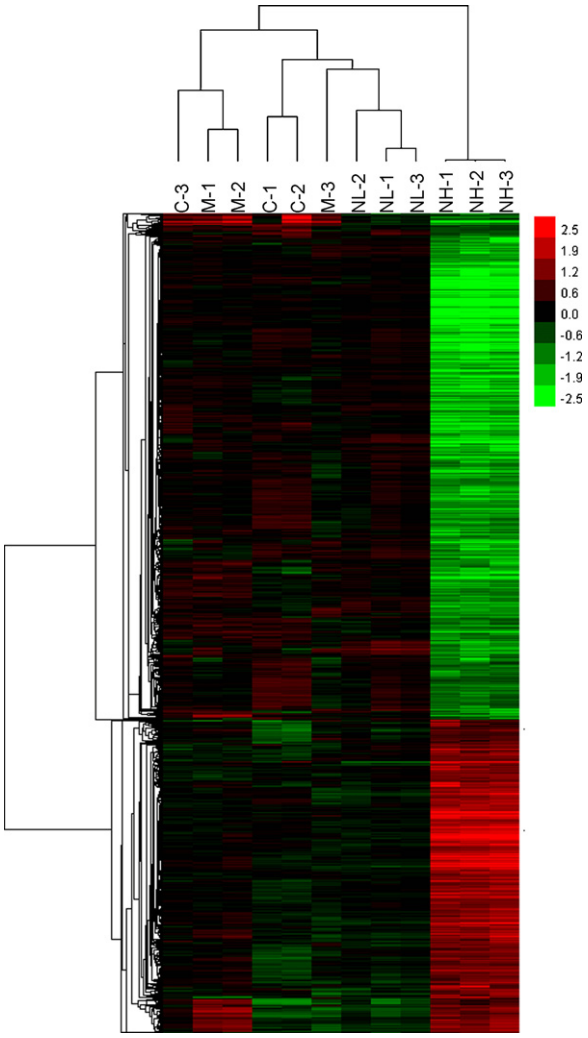


**Fig. 4 – Hierarchical clustering dendrogram comparison of all micro-copper- or nano-copper-altered groups to vehicle control exposure. Each sample listed contains the average gene expression value for three replicates. C: vehicle control, M: microcoppers 200 mg/kg, NL: nanocoppers 100 mg/kg, NH: nanocoppers 200 mg/kg.**

### 3.6. *Hierarchical cluster analysis*

Genes were selected for clustering if their expression was 2-fold greater or 2-fold less with treatment, relative to control (Fig. 4). The vertical axis shows the clustering of genes according to their expression profile in the treatment. The horizontal axis shows the clustering according to the expression across

treatments. From the horizontal axis, we found that the clustering reflected the degree of renal injury in the different groups. The greatest distance of the node was between the control and 200 mg/kg nanocopper, whereas the vehicle control and microcopper-treated groups clustered together. Thus, the gene expression patterns in nanocopper-treated kidneys are dramatically different than microcopper-treated kidneys, which are similar to the vehicle control group.

### 3.7. *Gene ontology and pathway enrichment*

The genes altered by treatment with microcopper and nanocopper at different doses could be divided into several large functional categories according to gene ontology and pathway analysis (Tables 6 and 7). Among the samples from nanocopper-treated rats (200 mg/kg/day), which showed obvious phenotypes, the largest category in GO Molecular Function was iron ion binding, in GO Biology Process was electron transport, and in GO Cell Component was mitochondrion and endoplasmic reticulum. In KEGG analysis, the largest pathways significantly affected in the 200 mg/kg nanocopper group were involved in valine, leucine, and isoleucine degradation, complement and coagulation cascades, oxidative phosphorylation, cell cycle, fatty acid metabolism, and the mitogen-activated protein kinase (MAPK) signaling pathway. Other significantly induced genes were involved in metabolism of xenobiotics by cytochrome P450, tryptophan metabolism, glycolysis/gluconeogenesis, glutathione metabolism, and extracellular matrix-receptor interaction. For the samples from nanocopper-treated rats (100 mg/kg) in which adverse effects were not obvious, a series of gene functional categories were found to be dramatically changed. Among them, the valine, leucine, and isoleucine degradation pathway and complement and coagulation cascades pathway were dramatically changed. However, in the microcopper-treated rats (200 mg/kg), no functional categories were significantly changed. Thus, we concentrated on the functional categories that were dramatically changed in the two dose groups, as well as the categories changed in the high dose (200 mg/kg/day) group.

### 3.8. *Real-time quantitative PCR analysis*

Expression of select genes that were differentially increased or decreased with microarray analysis, including *Kim*-1(kidney injury molecule 1), *Gpx*2(glutathione peroxidase 2), *Hspa*1a(heat shock 70 kD protein 1A), *G6pc*(glucose-6-phosphatase, catalytic), *Rgn*(regucalcin), and F2(coagulation factor II), was confirmed with real-time RT–PCR analysis using SYBR Green (Fig. 5). The trend of the changes in gene expression levels was closely correlated to the corresponding microarray data, although the exact fold change was different between these two assays. Overall, we were able to confirm gene expression profiles measured by microarray analysis using real-time RT–PCR. These data indicate that our strict criteria for determining differentially expressed genes with microarray resulted in detection of meaningful changes.

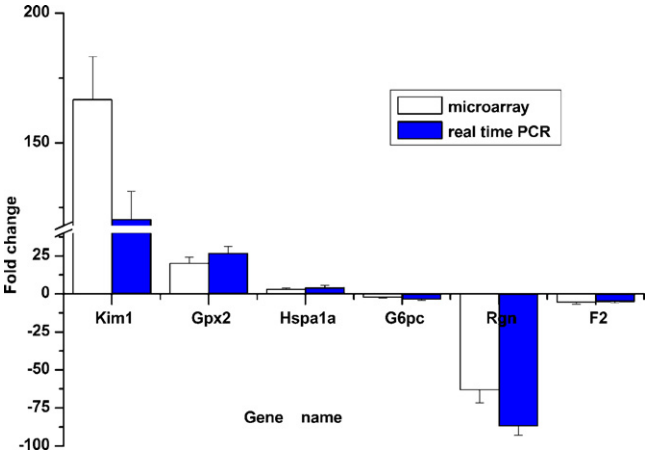


**Fig. 5 – Fold change of selected genes in nanocoppers 200 mg/kg group using microarray and real-time PCR.**

## 4. Discussion

Here, we found that nanocopper exhibits overt toxicity after being orally administered to male Wistar rats at 200 mg/kg daily for 5 days. As a target organ, the kidney showed widespread necrosis of renal proximal tubule cells, but the same dosage of microcopper showed no effect on rat kidney. This toxicity was verified by conventional toxicological parameters, including BW, clinical chemistry, and histopathology. These findings are consistent with a previous acute toxicity study that classified nanocopper as a moderate toxicant (Chen et al., 2006; Meng et al., 2007). In addition, we used a transcriptomic approach to obtain a global view of the transcriptional response of the kidneys in nanocopper-treated rats and to gain insights into the molecular mechanisms of nanocopper-induced kidney injury.

Because toxicity is generally directly related to biological perturbation at the cellular level, increasing our knowledge of the cellular perturbations and the consequences to biological function is essential (Oberemm et al., 2005). Toxicogenomics provides new tools to explore the initial events of toxic phenomena because it provides information regarding changes that may occur at the molecular level before clinic signs become evident (Carlson and Silkworth, 2009). Our gene expression study indicated that a dose of nanocopper that results in structural and functional nephrotoxicity also causes a marked alteration in renal gene expression profiles in male Wistar rats. The number of differentially expressed genes was 2773 in high dose (200 mg/kg) nanocopper-treated rat kidney, which exhibited widespread renal proximal tubule necrosis. In low dose (100 mg/kg) nanocopper-treated rats in which only swelling of the proximal tubule epithelia was observed compared with vehicle control, 120 genes were dramatically changed. As expected, the number of significantly changed genes in microcopper-treated rats (200 mg/kg), which did not show any obvious changes in conventional parameters compared to the vehicle control group, was only two. There were 56 genes that were differentially regulated in both the 100 mg/kg and 200 mg/kg nanocopper-treated groups. Among them, a change in the expression of *Kim*-1 was one of the earliest

**Table 6 – Gene ontology classification of extracted probe sets (nanocoppers 200 mg/kg).**

| Term | Genes | P value |
|---|---|---|
| Molecular function | | |
| GO:0050660 FAD binding | 3 | 2.46E-2 |
| GO:0004869 cysteine protease inhibitor activity | 3 | 6.08E-3 |
| GO:0003755 peptidylprolyl cistrans isomerase activity | 3 | 2.94E-3 |
| GO:0004673 protein histidine kinase activity | 3 | 9.76E-3 |
| GO:0004740 [pyruvate dehydrogenase (lipoamide)] kinase activity | 3 | 5.73E-4 |
| GO:0050381 unspecific monooxygenase activity | 5 | 2.45E-3 |
| GO:0020037 heme binding | 9 | 1.08E-2 |
| GO:0005506 iron ion binding | 14 | 2.11E-3 |
| Biology process | | |
| GO:0009615 response to virus | 3 | 1.56E-3 |
| GO:0006805 xenobiotic metabolism | 3 | 5.33E-4 |
| GO:0018106 peptidyl-histidine phosphorylation | 3 | 1.88E-3 |
| GO:0008272 sulfate transport | 3 | 1.41E-4 |
| GO:0006118 electron transport | 17 | 1.11E-4 |
| Cell component | | |
| GO:0005640 nuclear outer membrane | 3 | 3.0E-6 |
| GO:0005792 microsome | 9 | 2.94E-3 |
| GO:0005783 endoplasmic reticulum | 13 | 1.76E-2 |
| GO:0005739 mitochondrion | 18 | 1.95E-3 |

and most prominent effects observed in kidneys. *Kim*-1 is a member of a gene family encoding T-cell immunoglobulin mucin proteins and is involved in immune regulation and renal tubule regeneration after ischemic- or nephrotoxicant-induced injury (Han et al., 2002; Ichimura et al., 2004). *KIM*-1 is a phosphatidylserine receptor that allows tubule epithelial cells to recognize and internalize apoptotic bodies and cell debris, thus preventing tubule obstruction and facilitating remodeling and regeneration of the tubule epithelium in response to injury. Recently, several investigators have proposed *KIM*-1 to be an early biomarker of kidney toxicity (Bailly et al., 2002; Han et al., 2002; Amin et al., 2004).

### 4.1. *Valine, leucine, and isoleucine degradation*

Further gene ontology and pathway enrichment analyses indicated involvement of genes in valine, leucine, and isoleucine degradation, as well as complement and coagulation cascade pathways in nanocopper-induced kidney injury, which presented a dose response to nanocopper and might be useful as potential biomarkers. Leucine, isoleucine, and valine are branched-chain amino acids (BCAAs). They are considered essential because they cannot be synthesized de novo and must be obtained from the diet. They are necessary for protein and neurotransmitter synthesis. Leucine, isoleucine, and valine also are important sources of nitrogen for synthesis of nonessential amino acids, such as glutamine and alanine. There is increasing evidence of their pivotal role in regulating the anabolic process involving both protein synthesis and degradation. Furthermore, BCAAs are reported to spare lean body mass during weight loss (1), promote wound healing (2), promote muscle protein anabolism in muscle wasting with ageing (3), and have beneficial effects in the setting of renal and liver disease (Marchesini et al., 2003). There were 22 genes in this pathway that were dramatically changed including one that was upregulated and 21 that were downregulated, suggesting that protein and neurotransmitter synthesis in renal tubular epithelial cells may be significantly influenced by administration of nanocopper. The body initiates a defense reaction at the gene level to reduce adverse effects. Thus, because the nanocopper was orally gavaged, the ingestion of valine, leucine, and isoleucine from the diet in the rats may have decreased. Thus, to maintain functions such as protein and neurotransmitter synthesis, the body had to decrease the degradation of BCAAs by regulating related genes.

### 4.2. *Complement and coagulation cascades*

The complement and coagulation cascades pathway is another pathway that showed significant expression changes in both the 100 mg/kg and 200 mg/kg nanocopper groups. The convergence between complement and the clotting system extends far beyond the chemical nature of the complement and coagulation components, both of which are involved in proteolytic cascades. Complement effectors directly enhance coagulation. These effects are supplemented by the interactions of complement with other inflammatory mediators that increase the thrombogenicity of blood. In addition, complement inhibits anticoagulant factors (Markiewski et al., 2007). We found that some genes such as coagulation factor II (F2), complement component 1, s subcomponent (*C1s*), fibrinogen gamma chain (*Fgg*), and plasminogen (*Plg*), which play an important role in blood clotting, were dramatically downregulated, resulting in decreased coagulation. The F2 gene encodes a protein called prothrombin (also called coagulation factor II), which circulates in the bloodstream in an inactive form until an injury occurs that damages blood vessels. In response to injury, prothrombin is converted to its active form, thrombin. Thrombin then converts fibrinogen into fibrin, the primary protein that makes up blood clots. Thrombin is also thought to be involved in cell growth and division (proliferation), tissue repair, and the formation of new blood vessels (angiogenesis) (Markiewski et al., 2007). Thus, copper nanoparticles may play

**Table 7 – KEGG pathway classification of extracted probe sets(nanocoppers 200 mg/kg).**

| Category | Pathway name | Genes | P value |
|---|---|---|---|
| *Metabolism* | | | |
| Carbohydrate metabolism | Glycolysis/gluconeogenesis | 15 | 2.0E-6 |
| | Propanoate metabolism | 14 | 0.0 |
| | Pyruvate metabolism | 11 | 0.0 |
| | Butanoate metabolism | 10 | 2.0E-6 |
| | Citrate cycle (TCA cycle) | 9 | 0.0 |
| | Fructose and mannose metabolism | 8 | 3.21E-3 |
| | Starch and sucrose metabolism | 6 | 1.89E-3 |
| | Galactose metabolism | 6 | 8.94E-3 |
| Energy metabolism | **Oxidative phosphorylation** | **21** | **0.0** |
| | Nitrogen metabolism | 10 | 1.0E-6 |
| Lipid metabolism | Fatty acid metabolism | 21 | 0.0 |
| | Arachidonic acid metabolism | 13 | 9.7E-5 |
| | Linoleic acid metabolism | 9 | 4.34E-4 |
| | Glycerolipid metabolism | 8 | 3.5E-4 |
| | Bile acid biosynthesis | 7 | 1.45E-4 |
| | Biosynthesis of steroids | 7 | 3.0E-6 |
| | Fatty acid elongation in mitochondria | 6 | 4.0E-6 |
| Nucleotide metabolism | Purine metabolism | 14 | 1.84E-3 |
| | Pyrimidine metabolism | 7 | 8.47E-3 |
| Amino acid metabolism | **Valine, leucine and isoleucine degradation** | **22** | **0.0** |
| | Tryptophan metabolism | 16 | 0.0 |
| | Glycine, serine and threonine metabolism | 15 | 0.0 |
| | Cysteine metabolism | 11 | 0.0 |
| | Arginine and proline metabolism | 11 | 1.0E-5 |
| | Lysine degradation | 10 | 0.0 |
| | Urea cycle and metabolism of amino groups | 10 | 1.0E-6 |
| | Glutamate metabolism | 10 | 6.38E-4 |
| Amino acid metabolism | Alanine and aspartate metabolism | 8 | 0.0 |
| | Histidine metabolism | 6 | 2.51E-4 |
| | Methionine metabolism | 6 | 2.2E-5 |
| Metabolism of other amino acids | **Glutathione metabolism** | **14** | **0.0** |
| | Beta-Alanine metabolism | 8 | 2.0E-6 |
| | Selenoamino acid metabolism | 6 | 3.96E-4 |
| Xenobiotics biodegradation and metabolism | Metabolism of xenobiotics by cytochrome P450 | 18 | 0.0 |
| | Caprolactam degradation | 6 | 4.0E-6 |
| *Environmental information processing* | | | |
| Signal transduction | **MAPK signaling pathway** | **20** | **4.66E-2** |
| | TGF-beta signaling pathway | 9 | 1.44E-2 |
| Signaling molecules and interaction | ECM-receptor interaction | 14 | 2.06E-3 |
| *Cellular processes* | | | |
| Cell growth And death | **Cell cycle** | **21** | **0.0** |
| Cell communication | Gap junction | 9 | 3.36E-2 |
| Endocrine system | Insulin signaling pathway | 13 | 1.18E-2 |
| | Adipocytokine signaling pathway | 10 | 1.74E-2 |
| Immune system | **Complement and coagulation cascades** | 11 | 5.5E-5 |
| | Antigen processing and presentation | 9 | 4.09E-2 |
| | Hematopoietic cell lineage | 9 | 3.1E-2 |
| *Human diseases* | | | |
| Neurodegenerative diseases | Alzheimer's disease | 7 | 4.77E-4 |

Bold pathways were discussed in details in the discussion.

a role in anticoagulation in nanocopper-administered rats, a hypothesis that requires validation at the protein level.

### 4.3. *Oxidative phosphorylation*

Genes changed in the group receiving the high dose (showing an obvious phenotypes) were functionally categorized. A high number of affected genes related to metabolism, cellular processes, and environmental information processing were among those involved in the development of the observed phenotypes. We focused on mitochondrial energetic pathways and demonstrated that a widespread suppression of the mitochondrial energy production system and transcription co-activator factors that regulate mitochondrial genes involved in substrate metabolism and oxidative phosphorylation (OxPhos) occurs at the transcriptional level. These changes were associated with reduced activities of Complex I and V of the OxPhos pathway, which translated into diminished capacity of renal mitochondria to utilize oxygen and produce ATP from ADP. Complex I of the electron transport chain, which is composed of three subcomplexes (I$\alpha$, I$\beta$, and I$\lambda$) with 14 central and 32 accessory subunits (Brandt, 2006),

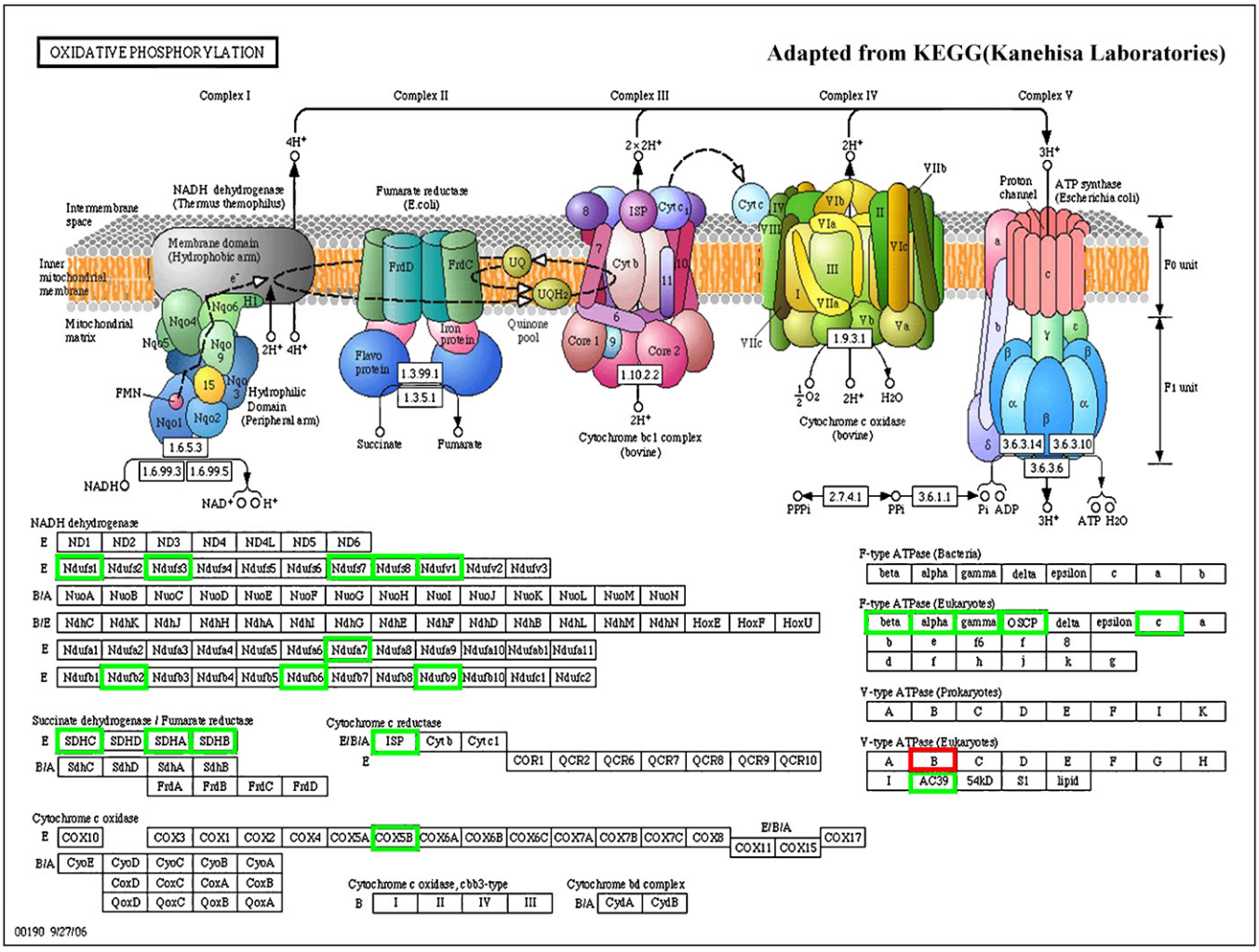


**Fig. 6 – Gene expression changes involved in the oxidative phosphorylation regulation. There are 20 genes were down-regulated (green), while only one gene was up-regulated (red) in this pathway. (For interpretation of the references to colour in this figure legend, the reader is referred to the web version of this article.)**

harbors NADH dehydrogenase and oxidoreductase activities and catalyzes the first step of NADH oxidation to transfer electrons from NADH and flavin mononucleotide (derived from the tricarboxylic acid (TCA) cycle) to the respiratory chain. We found that 9 of the 46 genes that code for complex I subunits were dramatically downregulated (Fig. 6). Mitochondrial F0F1 ATP synthase (Complex V) catalyzes ATP synthesis by utilizing the electrochemical gradient generated by proton efflux across the inner membrane during electron transfer (Walker and Dickson, 2006). Complex V is composed of two linked multisubunit complexes: F0, the integral membrane-spanning component comprising the proton channel, and F1, the catalytic portion of mitochondrial ATP synthase, which is linked by a central and peripheral stalk (Carbajo et al., 2005; Walker and Dickson, 2006). We found that seven genes that code for subunits of complex V, including one that was upregulated and six that were downregulated, were significantly changed in rat kidney (Fig. 6). Genes in other metabolic pathways including fatty acid metabolism, glycolysis/gluconeogenesis, nitrogen metabolism, and the TCA cycle were significantly changed. Glucose-6-phosphatase (*G6PC*) catalyzes the terminal step in gluconeogenesis and glycogenolysis and is a key enzyme in glucose homeostasis. Downregulation of this gene was reported by Amin et al. (2004) and may suggest changes in cellular energy requirements during the acute phase of renal injury. Because tubular epithelia have a strong energy demand during normal function, this result strongly suggests that disruption and impairment of energy metabolism may be mechanistically linked to nanocopper-induced nephrotoxicity.

### 4.4. *Cell cycle*

Chemical injury may induce cell death in the renal proximal tubule epithelium, leading to cell dedifferentiation, migration, proliferation, and finally redifferentiation to restore a fully functional epithelial barrier (Bonventre, 2003). Cell cycling is essential for cell growth and proliferation. We found that 21 genes in the cell cycle pathway, including 20 that were upregulated and one that was downregulated, were differentially expressed. In particular, the genes *Ccna2*, *Ccnb1/2*, *MCM*, and *Chk1* play important roles in cell proliferation and

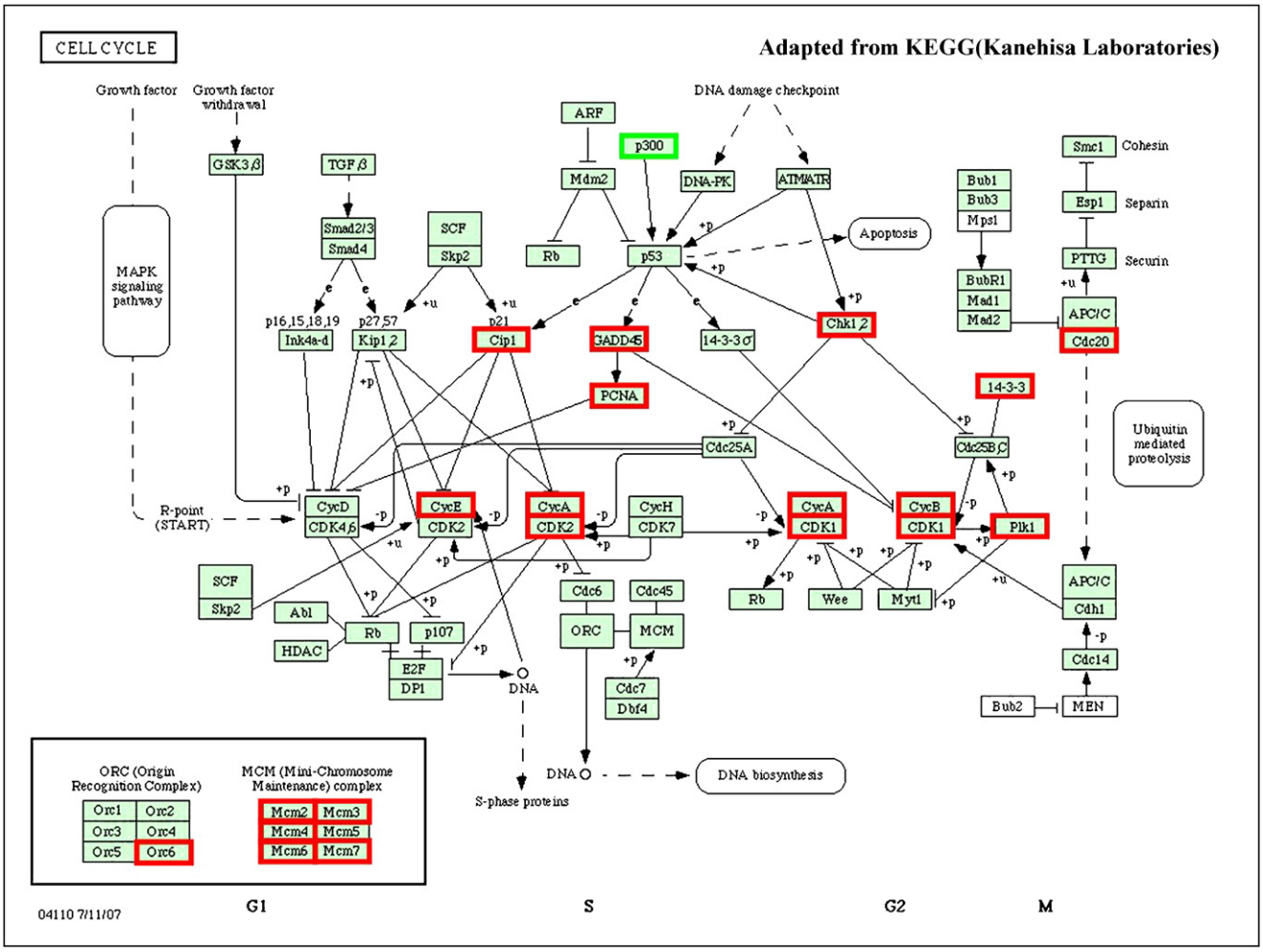


**Fig. 7 – Gene expression changes involved in the cell cycle regulation. There are 18 genes were up-regulated (green), while only one gene was down-regulated (red) in this pathway. (For interpretation of the references to colour in this figure legend, the reader is referred to the web version of this article.)**

were dramatically increased (Fig. 7). Cell cycle transitions are controlled by the enzymatic activity of complexes composed of cyclins and cyclin-dependent kinases (CDKs) (Grana and Reddy, 1995). Among the cyclins, cyclin A2 is unique in that it regulates progression through two critical transitions: cyclin A2/CDK2 controls the G1/S transition into DNA synthesis, and cyclin A2/CDK1 controls the G2/M entry into mitosis (Pagano et al., 1992). Cyclins B1 and B2 interact with CDK1 (Draetta et al., 1989; Pines and Hunter, 1989) but can also bind to CDK2 (Aleem et al., 2005). CDK1/cyclin B1 complexes promote nuclear envelope breakdown, chromosome condensation, and mitotic spindle assembly. Cytoplasmic CDK1/cyclin B2 complexes are essential for the mitotic reorganization of the Golgi apparatus (Draviam et al., 2001). The initiation of DNA replication in eukaryotic cells is a carefully regulated process requiring the orchestrated assembly of many proteins at origin sites, including the origin recognition complex and minichromosome maintenance (MCM) complex. The MCM complex consists of 6 subunits, MCM2 through 7, which form a hexamer. The MCM proteins are tightly regulated to prevent inappropriate DNA replication. The nuclear localization of the MCM2–7 complex is regulated by CDKs. MCM2–7 are imported into the nucleus when CDK activity is low in early G1 and exported from the nucleus during S phase when CDK activity is high (Labib et al., 2000; Nguyen et al., 2001). In our study, MCM2, MCM3, MCM4, MCM6, and MCM7 were all significantly upregulated, but MCM5 was not (Fig. 7). In response to DNA damage, cells activate a checkpoint pathway that arrests the cell cycle to provide time for repair and induces the transcription of genes that facilitate repair. Chk1 is a critical messenger of checkpoint control that is activated in response to diverse genotoxic insults. Together with Chk2, it regulates fundamental cellular functions such as DNA replication, cell cycle progression, chromatin restructuring, and apoptosis. Other dramatically changed genes that are involved in the DNA damage response include *CDKn*1a (Cyclin-dependent kinase inhibitor 1A), *Pdrg*1 (p53 and DNA damage regulated 1), and *Gadd*45a (Growth arrest and DNA damage-induced 45, Alpha). The significant increase in the expression of these genes that we observed indicates that the DNA in renal tubular epithelial cells may be severely damaged.

### 4.5. MAPK signaling pathway

MAPKs including extracellular signal-regulated kinase (ERK), c-Jun NH2-terminal kinase/stress-activated protein kinase (JNK/SAPK), and p38 are members of a family of serine–threonine kinases that participate in many cellular responses such as inflammation, cell growth, differentiation, and apoptosis (Cuschieri and Maier, 2005). One mechanism by which the transcription of detoxification genes is activated is via MAPK pathways (Galcheva-Garzova et al., 1994; Kyriakis and Avruch, 1996). Once activated, ERK, JNK, and p38 phosphorylate many proteins and transcription factors, resulting in the enhancement of the transcriptional activity of a multitude of genes (Karin, 1995). This mechanism was also suggested by the observations in our study. We found that many genes involved in the MAPK signaling pathway were dramatically changed. Heat shock 70-kDa protein 1A (hspa1a) plays a role in suppressing several apoptotic signaling pathways, including caspase cascades and stress-activated MAPK pathways that include the JNK and p38 signaling cascades (Gabai et al., 2000). These results further support a role for copper-induced stress as an activator of the MAPK signaling cascade. In addition to MAPK signaling pathways, our results indicate that nanocopper can influence the TGF-beta and insulin signaling pathways. The role of these pathways in nanocopper-related nephrotoxicity remains unclear and requires further investigation.

### 4.6. Glutathione metabolism and oxidative stress

Downregulation of the pathways related to the oxidative stress response, including glutathione metabolism and antioxidant genes, may also be related to the mechanism of nanocopper-induced renal injury. Glutathione is the most abundant antioxidant in cells, where it is formed predominantly in two redox forms: reduced (GSH) and oxidized (GSSG). Glutathione and glutathione-associated metabolism provide the major line of defense for protecting cells from oxidative and other forms of stress (Hayes and McLellan, 1999). Besides its function as an intracellular redox buffer, GSH plays multiple roles in cell physiology, detoxification of toxic chemicals and electrophiles, and regulation of cell death. Data from the last few years also support the idea that a decrease in GSH is often associated with the apoptotic program. GSH functions not only as an antioxidant itself, but also as a component of the detoxifying enzyme system. Glutathione-S-transferase (GST) plays a critical role in defending the organism against reactive electrophiles by removing them through conjugation with GSH (Maher, 2005). In addition to the functions of GSH itself, the GSH/GSSG redox couple acts to maintain the redox environment of the cell. This observation may have important implications in nanocopper-induced nephrotoxicity, because the glutathione production pathway can be considered as a first-line defense against oxidative stress, a common toxicological mechanism leading to cell death. Glutathione peroxidase (GPX), an important antioxidant enzyme, breaks down hydrogen peroxide (Gomes-Junior et al., 2006) and is closely involved in glutathione enzymatic changes (Swiergosz-Kowalewska et al., 2006). GPX activity is believed to play an important role in cellular antioxidant defense by reducing hydrogen peroxide and various hydroperoxides to water using glutathione as a reducing agent (Wendel, 1980). Heme oxygenase-1 (Hmox1), which oxidatively cleaves heme to produce biliverdin, is a well-known biomarker of oxidative stress and is induced in animal cells by inorganic mercury (Park and Park, 2007). Thioredoxin reductase (Txnrd) and catalase (Cat) are also clear biomarkers of oxidative stress (Hansen et al., 2006; Margonis et al., 2007). Downregulation of Txnrd increases the level of oxidized thioredoxin, which is a regulatory apparatus for oxidative injury in mitochondria, and leads to increased susceptibility to cell death (Das, 2005). In our study, these genes were all dramatically changed.

### 4.7. Physicochemical parameters relating to nanotoxicity

One important issue in nanotoxicology is assessing what kind of physicochemical parameters are related to the nanotoxicity. Kirchner et al. (2005) distinguished three main causes of nanoparticle toxicity following contact with live cells. The first is due to the chemical toxicity of materials from which they were made, the second is due to their small size, and the third is due to their shape. For nanocopper, the unique electron structure of copper allows direct interaction with spin-restricted molecular oxygen, thus enabling copper to participate as a protein cofactor in fundamental redox reactions. Many types of enzymes exploit copper chemistry to catalyze such reactions, including cytochrome oxidase, superoxide dismutase, lysyl oxidase, and ceruloplasmin. The expression of genes coding for these proteins, such as cytochrome P450 3a13 (*Cyp3a13*, 26.56), cytochrome P450 1a1 (*Cyp1a1*, 0.31), superoxide dismutase 1(*Sod1*, 0.44), copper chaperone for superoxide dismutase (*Ccs*, 0.45), lysyl oxidase (*Lox*, 2.98), and ceruloplasmin (*Cp*, 2.83), changed dramatically. Thus, copper ions are essential in cellular respiration, antioxidant defense, neurotransmitter function, connective tissue biosynthesis, and cellular iron metabolism. Proteins utilize the redox nature of copper to facilitate electron transfer reactions and to bind reactive intermediates and avoid their reactivity (Linder and Hazegh-Azam, 1996). Nevertheless, the chemical properties that make copper biologically useful are also potentially toxic. On the other hand, in accordance with the collision theory in chemistry, a huge specific surface area leads to a high probability of effective collision, which determines the ultrahigh reactivity during molecular interactions. Some chemical reactions are allowed in terms of chemical thermodynamics but could not happen in terms of reaction kinetics. However, when particles are reduced in size to nano-scale, the huge specific surface area will sharply accelerate chemical reactions and may eventually cause nanotoxicity that micro-scale copper particles do not have (Meng et al., 2007).

The gene expression analysis presented in this paper represents a snapshot of events after five days of treatment. Not all changes in cellular mechanisms can be measured at the gene expression level. Protein modification and subcellular redistribution of proteins provide an organism with rapid mechanisms to respond to stimuli without the need to change gene expression. The mRNA level of a gene does not always correlate with the amount of translated protein, which in turn is not necessarily proportional to the protein activity.

In fact, several studies have reported that mRNA expression correlates poorly with protein expression (Chen et al., 2002; Greenbaum et al., 2003; Gygi et al., 1999). Thus, in parallel with gene expression experiments, we are performing proteomic investigations for protein profiling nanocopper-treated rat kidneys, and the data obtained will be analyzed together to achieve a better mechanistic understanding of the toxicological response to nanocopper.

## 5. Conclusions

Our study found that nanocopper compared to microcopper at the same dosage can induce nephrotoxicity of rats repeatedly treated with an oral dose of 200 mg/kg/d, which can be demonstrated by traditional toxicological results including BW loss, significant changes in clinic chemistry parameters, and widespread renal proximal tubule necrosis. The dramatically changed genes are involved in metabolism, cellular processes, and environmental information processing, especially valine, leucine, and isoleucine degradation, complement and coagulation cascades, oxidative phosphorylation, cell cycling, MAPK signaling, and glutathione metabolism and are considered to be related to the nephrotoxicity. Our results also suggest that altered gene expression patterns induced by exposure to a low dose of one potentially toxic nanomaterial may reveal signs of cell stress or subtle cell injury indicative of overt toxicity at higher doses. Thus, the use of a systems toxicology approach to study the toxicity of nanomaterials whose prior knowledge is limited is likely to yield valuable insight.

## Conflict of interest

The authors declare that there are no conflicts of interest.

## Acknowledgments

We thank Prof. Yuliang Zhao (National Center for Nanoscience and Technology of China, Chinese Academy of Sciences, China) for technical assistance on the physicochemical characterization of copper particles, and Drs. Xiaohong Chen and Haiyan Shen (CapitalBio Corporation, China) for their kind help in gene expression analyses.

This work was supported by the National Basic Research Program of China (2006CB705602), National Grand Science and Technology Special Program for Innovation of New Drugs (2008ZX09305-003), National Natural Science Foundation (81001254), Beijing Natural Science Foundation (7092079), and Beijing Science Foundation (Z08030203080818).

## Appendix A. Supplementary data

Supplementary data associated with this article can be found, in the online version, at doi:10.1016/j.etap.2011.05.014.

## REFERENCES

Aguar-Fernandez, M.A., Hullmann, A., 2007. A boost for safer nanotechnology. Nano Today 2, 56.

Aleem, E., Kiyokawa, H., Kaldis, P., 2005. Cdc2-cyclin E complexes regulate the G1/S phase transition. Nat Cell Biol. 7, 831–836.

Amin, R.P., Vickers, A.E., Sistare, F., Thompson, K.L., Roman, R.J., Lawton, M., Kramer, J., Hamadeh, H.K., Collins, J., Grissom, S., et al., 2004. Identification of putative gene based markers of renal toxicity. Environ. Health Perspect. 112, 465–479.

Bailly, V., Zhang, Z., Meier, W., Cate, R., Sanicola, M., Bonventre, J.V., 2002. Shedding of kidney injury molecule-1, a putative adhesion protein involved in renal regeneration. J. Biol. Chem. 277, 39739–39748.

Bonventre, J.V., 2003. Dedifferentiation and proliferation of surviving epithelial cells in acute renal failure. J. Am. Soc. Nephrol. 14 (Suppl. 1), S55–S61.

Brandt, U., 2006. Energy converting NADH: quinone oxidoreductase (Complex I). Annu. Rev. Biochem. 75, 69–92.

Carbajo, R.J., Kellas, F.A., Runswick, M.J., Montgomery, M.G., Walker, J.E., Neuhaus, D., 2005. Structure of the F1-binding domain of the stator of bovine F1Fo-ATPase and how it binds an alpha-subunit. J. Mol. Biol. 351, 824–838.

Carlson, E.A., Silkworth, J.B., 2009. Toxicogenomics in human health risk assessment. Toxicol. Appl. Pharmacol. 236, 254–256.

Chen, G., Gharib, T.G., Huang, C.C., Taylor, J.M., Misek, D.E., Kardia, S.L., Giordano, T.J., Iannettoni, M.D., Orringer, M.B., Hanash, S.M., 2002. Discordant protein and mRNA expression in lung adenocarcinomas. Mol. Cell. Proteomics 1, 304–313.

Chen, Z., Meng, H., Xing, G.M., Chen, C.Y., Zhao, Y.L., Jia, G., Wang, T.C., Yuan, H., Ye, C., Zhao, F., Chai, Z.F., Zhu, C.F., Fang, X.H., Ma, B.C., Wan, L.J., 2006. Acute toxicological effects of copper nanoparticles in vivo. Toxicol. Lett. 163, 109–120.

Cioffi, N., Ditaranto, N., Torsi, L., Picca, R.A., Sabbatini, L., Valentini, A., Novello, L., Tantillo, G., Bleve-Zacheo, T., Zambonin, P.G., 2005. Analytical characterization of bioactive fluoropolymer ultra-thin coatings modified by copper nanoparticles. Anal. Bioanal. Chem. 381 (3), 607–616.

Cuschieri, J., Maier, R.V., 2005. Mitogen-activated protein kinase (MAPK). Crit. Care Med. 33, S417–S419.

Das, K.C., 2005. Thioredoxin and its role in premature newborn biology. Antioxid. Redox Signal. 7, 1740–1743.

Donaldson, K., Aitken, R., Tran, L., Stone, V., Duffin, R., Forrest, G., Alexander, A., 2006. Carbon nanotubes: a review of their properties in relation to pulmonary toxicology and workplace safety. Toxicol. Sci. 92, 5–22.

Draetta, G., Luca, F., Westendorf, J., Brizuela, L., Ruderman, J., Beach, D., 1989. Cdc2 protein kinase is complexed with both cyclin A and B: evidence for proteolytic inactivation of MPF. Cell 56, 829–838.

Draviam, V.M., Orrechia, S., Lowe, M., Pardi, R., Pines, J., 2001. The localization of human cyclins B1 and B2 determines CDK1 substrate specificity and neither enzyme requires MEK to disassemble the Golgi apparatus. J. Cell Biol. 152, 945–958.

Eisen, M.B., Spellman, P.T., Brown, P.O., Botstein, D., 1998. Cluster analysis and display of genome-wide expression patterns. Proc. Natl. Acad. Sci. 95, 14863–14868.

Gabai, V.L., Yaglom, J.A., Volloch, V., Meriin, A.B., Force, T., Koutroumanis, M., Massie, B., Mosser, D.D., Sherman, M.Y., 2000. Hsp72-mediated suppression of c-Jun N-terminal kinase is implicated in development of tolerance to caspase-independent cell death. Mol. Cell. Biol. 20, 6826–6836.

Galcheva-Garzova, Z., Derijard, B., Wu, J.H., Davis, R.J., 1994. An osmosensing signal transduction pathway in mammalian cells. Science 265, 806–808.

Gomes-Junior, R.A., Moldes, C.A., Delite, F.S., Pompeu, G.B., Grata, P.L., Mazzafera, P., Lea, P.J., Azevedo, R.A., 2006. Antioxidant metabolism of coffee cell suspension cultures in response to cadmium. Chemosphere 65, 1330–1337.

Grana, X., Reddy, E.P., 1995. Cell cycle control in mammalian cells: role of cyclins, cyclin dependent kinases (CDKs), growth suppressor genes and cyclin-dependent kinase inhibitors (CKIs). Oncogene 11, 211–219.

Greenbaum, D., Colangelo, C., Williams, K., Gerstein, M., 2003. Comparing protein abundance and mRNA expression levels on a genomic scale. Genome Biol. 4 (9), 117.

Griffit, R.J., Weil, R., Hyndman, K.A., Hyndman, K.A., Denslow, N.D., Powers, K., Taylor, D., Barber, D.S., 2007. Exposure to copper nanoparticles causes gill injury and acute lethality in zebrafish (Danio rerio). Environ. Sci. Technol. 41 (23), 8178–8186.

Griffit, R.J., Hyndman, K., Denslow, N.D., Barber, D.S., 2009. Comparison of molecular and histological changes in zebrafish gills exposed to metallic nanoparticles. Toxicol. Sci. 107 (2), 404–415.

Gygi, S.P., Rochon, Y., Franza, B.R., Aebersold, R., 1999. Correlation between protein and mRNA abundance in yeast. Mol. Cell. Biol. 19, 1720–1730.

Han, W.K., Bailly, V., Abichandani, R., Thadhani, R., Bonventre, J.V., 2002. Kidney Injury Molecule-1 (KIM-1): a novel biomarker for human renal proximal tubule injury. Kidney Int. 62, 237–244.

Hansen, J.M., Zhang, H., Hones, D.P., 2006. Differential oxidation of thioredoxin-1, thioredoxin-2, and glutathione by metal ions. Free Radic. Biol. Med. 40, 138–145.

Hayes, J.D., McLellan, L.I., 1999. Glutathione and glutathione-dependent enzymes represent a coordinately regulated defence against oxidative stress. Free Radic. Res. 31, 273–300.

Ichimura, T., Hung, C.C., Yang, S.A., Stevens, J.L., Bonventre, J.V., 2004. Kidney injury molecule-1: a tissue and urinary biomarker for nephrotoxicant-induced renal injury. Am. J. Physiol. Renal Physiol. 286, F552–F563.

Karin, M., 1995. The regulation of AP-1 activity by mitogen-activated protein kinases. J. Biol. Chem. 270, 16483–16486.

Kirchner, C., Liedl, T., Kudera, S., Pellegrino, T., Javier, A.M., Gaub, H.E., Stölzle, S., Fertig, N., Parak, W.J., 2005. Cytotoxicity of colloidal CdSe and CdSe/ZnS nanoparticles. Nano Lett. 5, 331–338.

Kyriakis, J.M., Avruch, J., 1996. Protein kinase cascades activated by stress and inflammatory cytokines. Bioessays 18, 567–577.

Labib, K., Tercero, J.A., Diffley, J.F., 2000. Uninterrupted Mcm2-7 function required for DNA replication fork progression. Science 288, 1643–1647.

Lewinski, N., Colvin, V., Drezek, R., 2008. Cytotoxicity of nanoparticles. Small 4, 26–49.

Linder, M.C., Hazegh-Azam, M., 1996. Copper biochemistry and molecular biology. Am. J. Clin. Nutr. 63, 797S–811S.

Liu, G., Li, X., Qin, B., Xing, D., Guo, Y., Fan, R., 2004. Investigation of the mending effect and mechanism of copper nanoparticles on a tribologically stressed surface. Tribology Lett. 17, 961–966.

Maher, P., 2005. The effects of stress and aging on glutathione metabolism. Ageing Res. Rev. 4, 288–314.

Mann S. 2006. Nanotechnology and Construction. Nanoforum Report. Institute of Nanotechnology, Stirling.

Marchesini, G., Bianchi, G., Merli, M., Amodio, P., Panella, C., Loguercio, C., Rossi Fanelli, F., Abbiati, R., Italian, B.S.G., 2003. Nutritional supplementation with branchedchain amino acids in advanced cirrhosis: a double-blind, randomized trial. Gastroenterology 124, 1792–1801.

Margonis, K., Fatouros, I.G., Jamurtas, A.Z., Kikolaidis, M.G., Douroudos, I., Chatzinikolaou, A., Mitrakou, A., Mastorakos, G., Papassotiriou, I., Taxildaris, K., Kouretas, D., 2007. Oxidative stress biomarkers responses to physical overtraining: implications for diagnosis. Free Radic. Biol. Med. 43, 901–910.

Markiewski, M.M., Nilsson, B., Ekdahl, K.N., Mollnes, T.E., Lambris, J.D., 2007. Complement and coagulation: strangers or partners in crime? Trends Immunol. 28 (4), 184–192.

Medina, C., Santos-Martinez, M.J., Radomski, A., Corrigan, O.I., Radomski, M.W., 2007. Nanoparticles: pharmacological and toxicological significance. Br. J. Pharmacol. 150, 552–558.

Meng, H., Chen, Z., Xing, G.M., Yuan, H., Chen, C.Y., Zhao, F., Zhang, C.C., Zhao, Y.L., 2007. Ultrahigh reactivity provokes nanotoxicity: explanation of oral toxicity of nano-copper particles. Toxicol. Lett. 175, 102–110.

Nguyen, V.Q., Co, C., Li, J.J., 2001. Cyclin-dependent kinases prevent DNA re-replication through multiple mechanisms. Nature 411, 1068–1073.

Oberemm, A., Onyon, L., Gundert-Remy, U., 2005. How can toxicogenomics inform risk assessment? Toxicol. Appl. Pharmacol. 207, S592–S598.

Pagano, M., Pepperkok, R., Verde, F., Ansorge, W., Draetta, G., 1992. Cyclin A is required at two points in the human cell cycle. EMBO J. 11, 961–971.

Park, E.J., Park, K., 2007. Induction of reactive oxygen species and apoptosis in BEAS-2B cells by mercuric chloride. Toxicol. In Vitro 21, 789–794.

Pines, J., Hunter, T., 1989. Isolation of a human cyclin cDNA: evidence for cyclin mRNA and protein regulation in the cell cycle and for interaction with p34cdc2. Cell 58, 833–846.

Swiergosz-Kowalewska, R., Bednarska, A., Kafel, A., 2006. Glutathione levels and enzyme activity in the tissues of bank vole *Clethrionomys glareolus* chronically exposed to a mixture of metal contaminants. Chemosphere 65, 963–974.

Walker, J.E., Dickson, V.K., 2006. The peripheral stalk of the mitochondrial ATP synthase. Biochim. Biophys. Acta 1757, 286–296.

Wendel, A., 1980. Glutathione peroxidase. In: Jakoby, W.B. (Ed.), Enzymatic Basis of Detoxification, vol. 1. Academic Press, New York, NY, pp. 333–353.

Zweck, A., Bachmann, G., Luther, W., Ploetz, C., 2008. Nanotechnology in Germany: from forecasting to technological assessment to sustainability studies. J. Cleaner Prod. 16, 977–987.